

Infrared Spectra of the (AgCO)₂ and Ag_nCO (*n* = 2–4) Molecules in Rare-Gas Matrices

Ling Jiang and Qiang Xu*

*National Institute of Advanced Industrial Science and Technology (AIST), Ikeda, Osaka 563-8577, Japan, and Graduate School of Science and Technology, Kobe University, Nada Ku, Kobe, Hyogo 657-8501, Japan**Received: July 1, 2006; In Final Form: August 18, 2006*

Reactions of laser-ablated silver atoms with carbon monoxide molecules in solid argon and neon have been investigated using matrix-isolation IR spectroscopy. Small silver cluster carbonyls, (AgCO)₂ and Ag_nCO (*n* = 2–4), as well as mononuclear silver carbonyls, Ag(CO)₂ and Ag(CO)₃, are generated upon sample annealing in the argon experiments and are characterized on the basis of the isotopic substitution, the CO concentration change, and the comparison with theoretical predictions. However, these polynuclear carbonyls are absent from the neon experiments. Density functional theory calculations have been performed on these silver carbonyls and the corresponding ligand-free silver clusters, which support the identification of these silver carbonyls from the matrix IR spectrum. A terminal CO has been found in the most stable structures of (AgCO)₂, Ag₂CO, Ag₃CO, and Ag₄CO. Furthermore, a plausible reaction mechanism has been proposed to account for the formation of the (AgCO)₂ and Ag_nCO (*n* = 2–4) molecules.

Introduction

The interaction of silver atoms with small molecules (i.e., CO, O₂, CO₂, H₂, C₂H₄, etc.) is of considerable interest because of its importance in heterogeneous catalysis.¹ Silver clusters and small particles also play important roles in photography and new electronic materials.^{2,3} The reactions of silver atoms with oxygen molecules have been performed to understand their potential usefulness as localized bonding models for molecular dioxygen surface complexes, which are known to participate in silver-catalyzed oxidation reactions.⁴ Neutral and cationic silver carbonyls have been synthesized in low-temperature matrices, superacid solutions and in the presence of counteranions.^{5–9} Recently, the reactions of Cu, Ag, and Au atoms with a CO and O₂ mixture in solid argon have been studied, and it is found that the carbonyl metal oxides may act as the precursors for the oxidation of CO to CO₂.¹⁰ Extensive experimental and theoretical studies have also been performed to understand the properties of the silver clusters.^{11–13}

Among these small ligands, carbon monoxide is one of the most important in transition-metal chemistry from an academic or an industrial viewpoint.¹⁴ In the past 15 years, there has been a rapid development in the preparation and characterization of new homoleptic carbonyls of metals from groups 6 through 12, which are usually prepared using weakly coordinating anions, superacids, or strong acids.¹⁵ Recently, a series of cationic Ag_x-(CO)_n⁺ (1 ≤ *x* ≤ 15, *n* = 1–3) species were produced by electron impact ionization and mass spectrometrically identified but their structures were not characterized.¹⁶

Recent studies have shown that, with an aid of isotopic substitution technique, matrix isolation IR spectroscopy combined with quantum chemical calculation is very powerful in investigating the spectrum, structure, and bonding of novel species.^{17,18} Of particular interest is that the mononuclear metal complexes are favored under the experimental conditions of higher reagent concentration and lower laser energy, whereas the yields of the polynuclear metal complexes remarkably

increase with lower reagent concentration and higher laser energy. Taking the CO reagent as an example, some small metal cluster carbonyls, such as Fe₂CO,¹⁹ Co₂CO,²⁰ B₂CO, and B₂-(CO)₂,²¹ M₂CO (M = Sc, Y, and La),^{18c,22} Ti₂(CO)_n (*n* = 1, 2), and Ti₃(CO)_n (*n* = 1–3),²³ M_nCO (M = Si, Ge, Sn, Pb; *n* = 2–5),²⁴ and Au_nCO (*n* = 1–5) and Au₂(CO)₂,^{5e,25} have been synthesized via tuning the metal/CO ratios. In contrast with considerable studies of mononuclear silver carbonyls,⁵ however, much less work has been done on small silver cluster carbonyls. Here, we report a study of the reactions of laser-ablated silver atoms and small clusters with CO molecules in solid neon and argon. IR spectroscopy coupled with theoretical calculations provide evidence for the formation of (AgCO)₂ and Ag_nCO (*n* = 2–4) molecules.

Experimental and Theoretical Methods

The experiment for laser ablation and matrix isolation IR spectroscopy is similar to those previously reported.^{24d,26,27} Briefly, the Nd:YAG laser fundamental (1064 nm, 10 Hz repetition rate with 10 ns pulse width) was focused on the rotating Ag target. The laser-ablated Ag atoms were co-deposited with CO in excess neon (or argon) onto a CsI window cooled normally to 4 K (or 7 K) by means of a closed-cycle helium refrigerator. Typically, 1–15 mJ/pulse laser power was used. Carbon monoxide (99.95% CO), ¹³C¹⁶O (99%, ¹⁸O < 1%), and ¹²C¹⁸O (99%) were used to prepare the CO/Ne or CO/Ar mixtures. In general, matrix samples were deposited for 1 to 2 h with a typical rate of 2–4 mmol/h. After sample deposition, IR spectra were recorded on a BIO-RAD FTS-6000e spectrometer at 0.5 cm^{−1} resolution using a liquid-nitrogen-cooled HgCdTe (MCT) detector for the spectral range of 5000–400 cm^{−1}. Samples were annealed at different temperatures and subjected to broad-band irradiation (λ > 250 nm) using a high-pressure mercury arc lamp (Ushio, 100 W).

Quantum chemical calculations were performed to predict the structures and vibrational frequencies of the observed reaction products using the Gaussian 03 program.²⁸ The B3LYP and BPW91 density functional methods were used.²⁹ The

* To whom correspondence should be addressed. E-mail: q.xu@aist.go.jp.

TABLE 1: Infrared Absorptions (cm⁻¹) Observed after Co-deposition of Laser-Ablated Silver Atoms with CO in Excess Argon at 7 K

¹² C ¹⁶ O	¹³ C ¹⁶ O	¹² C ¹⁸ O	¹² C ¹⁶ O + ¹³ C ¹⁶ O	¹² C ¹⁶ O + ¹² C ¹⁸ O	R(12/13)	R(16/18)	assignment
2119.8	2072.9	2070.5	2120.1, 2072.9	2119.8, 2070.5	1.0226	1.0238	Ag ₄ CO
2113.8	2066.9	2064.3	2113.8, 2066.9	2113.8, 2064.3	1.0227	1.0240	Ag ₃ CO
2101.7	2055.2	2052.7	2101.8, 2055.1	2101.7, 2052.6	1.0226	1.0239	Ag ₃ CO
2077.0	2031.4	2027.9	2076.9, 2039.8, 2031.3; 2123.6 (sym)	2077.0, 2036.8, 2079.9; 2122.8 (sym)	1.0224	1.0242	(AgCO) ₂
1959.5	1916.1	1914.0	1959.6, 1941.2, 1927.5, 1916.2; 2077.6, 2062.6 (sym)	1959.5, 1940.4, 1925.9, 1914.1	1.0227	1.0238	Ag(CO) ₃
1842.1	1801.0	1799.5	1842.1, 1819.0, 1801.1; 2004.8 (sym)	1842.1, 1818.1, 1799.5; 2003.2 (sym)	1.0228	1.0237	Ag(CO) ₂
1826.7	1785.7	1785.9	1826.7, 1804.8, 1802.6, 1785.8; 1991.1, 1986.4 (sym)	1826.7, 1804.9, 1802.9, 1785.9; 1989.0, 1984.0 (sym)	1.0230	1.0228	Ag ₄ (CO) ₂ ⁺

TABLE 2: Comparison of Experimental and Calculated C–O Stretching Modes of the Silver Carbonyls

species	<i>ν</i> _{C–O} mode	experimental frequency (cm ⁻¹)	calculated frequency (cm ⁻¹)		
			B3LYP/6-311+G(d)-LANL2DZ	BPW91/6311+G(d)-LANL2DZ	BPW91/Aug-cc-PVTZ-LANL2DZ
Ag(CO) ₂	B ₂	1842.1	1998.3	1922.9	1922.3
Ag(CO) ₃	E	1959.5	2024.5	1970.2	1970.1
Ag ₂ CO	A	2113.8	2183.3	2059.4	2053.9
(AgCO) ₂	B _u	2077.0	2168.2	2042.5	2037.1
Ag ₃ CO	A ₁	2101.7	2121.5	2015.4	2016.4
Ag ₄ CO	A ₁	2119.8	2168.1	2056.2	2053.7

TABLE 3: Ground Electronic State, Point Group, Vibrational Frequencies (cm⁻¹), and Intensities (km/mol) of the Possible Reaction Products Calculated at the BPW91/Aug-cc-PVTZ-LANL2DZ Level

species	elec state	point group	frequency (intensity, mode)
Ag(CO) ₂	² A ₁	C _{2v}	2005.1 (0.5, A ₁), 1922.3 (2876, B ₂), 382.6 (18, B ₂), 303.2 (0.3, A ₁), 269.0 (23, B ₂), 200.1 (0.3, A ₁), 197.0 (0, A ₂), 90.1 (2, B ₁), 48.5 (1, A ₁)
Ag(CO) ₃	² A ₁ ''	D _{3h}	2053.2 (0, A ₁ '), 1970.1 (2058 × 2, E'), 367.6 (0.2 × 2, E''), 299.5 (0, A ₁ '), 260.1 (6 × 2, E'), 230.8 (0 × 2, E''), 217.5 (0, A ₂ '), 195.9 (10, A ₂ ''), 48.8 (1, A ₂ ''), 38.7 (0 × 2, E')
Ag ₂ CO	¹ A'	C _s	2053.9 (786, A'), 301.6 (15, A'), 204.1 (19, A'), 168.3 (2, A'), 152.7 (2, A'), 38.7 (0.8, A')
(AgCO) ₂	¹ A _g	C _{2h}	2052.2 (0, A _g), 2037.1 (1762, B _u), 310.6 (0, A _g), 288.4 (42, B _u), 211.3 (0, A _g), 192.8 (33, B _u), 162.3 (0, B _g), 157.2 (0, A _g), 141.9 (3, A _u), 49.5 (0, A _g), 28.0 (1, B _u), 5.6 (0, A _u)
AgAg(CO) ₂	¹ A ₁	C _{2v}	2042.5 (469, A ₁), 2015.6 (1446, B ₂), 374.4 (4, B ₂), 297.1 (4, A ₁), 255.7 (15, B ₂), 238.6 (0.2, A ₁), 223.0 (2, B ₁), 180.6 (0, A ₂), 162.0 (1, A ₁), 57.2 (0.2, A ₁), 44.5 (0.3, B ₁), 32.5 (0, B ₂)
Ag ₃ CO	² B ₂	C _{2v}	2016.4 (2243, A ₁), 303.9 (2, A ₁), 214.1 (1, B ₁), 195.3 (4, B ₂), 161.9 (2, A ₁), 102.6 (2, B ₂), 100.1 (0.1, A ₁), 34.3 (0.1, B ₁), 26.3 (0, B ₂)
Ag ₄ CO	¹ A ₁	C _{2v}	2053.7 (1091, A ₁), 306.6 (4, A ₁), 257.6 (1, B ₂), 206.7 (1, B ₁), 168.2 (0.1, A ₁), 160.9 (4, B ₂), 102.0 (0.1, A ₁), 100.6 (0, B ₂), 80.5 (2, A ₁), 34.8 (0, B ₁), 28.4 (0, B ₁), 20.2 (0, B ₂)

6-311+G(d) and Aug-cc-PVTZ basis sets were used for C and O atoms,³⁰ and the Los Alamos ECP plus DZ (LANL2DZ) basis set was used for Ag atoms.³¹ Geometries were fully optimized and vibrational frequencies were calculated with analytical second derivatives. The previous investigations have shown that such computational methods can provide reliable information for silver carbonyls, such as IR frequencies, relative absorption intensities, and isotopic shifts.⁵

Results and Discussion

Experiments have been done with carbon monoxide concentrations ranging from 0.02 to 0.4% in neon and argon. Recently, neon matrix investigations of the reaction of laser-ablated Ag atoms and CO molecules have characterized the mononuclear silver carbonyls, Ag(CO)_{*n*} (*n* = 2, 3) and Ag(CO)_{*n*}⁺ (*n* = 1–3).^{5c} In the more dilute CO circumstance relative to the previous experiment,^{5c} new absorptions of polynuclear silver carbonyls have been observed in the present argon experiments but not observed in neon. Typical IR spectra for the reactions of laser-ablated silver atoms with CO molecules in excess argon in the selected regions are shown in Figures 1–4, and the absorption bands in different isotopic experiments are listed in Table 1. The stepwise annealing and photolysis behavior of the product absorptions is also shown in the figures and will be discussed below. Experiments were also done with different concentrations of CCl₄ serving as an electron scavenger.

Quantum chemical calculations have been carried out for the possible isomers and electronic states of the potential product molecules. Calculated C–O stretching modes with different functional methods and basis sets have been compared with the experimental values in Table 2. Note that the calculated frequencies at the BPW91/6-311+G(d)-LANL2DZ and BPW91/Aug-cc-PVTZ-LANL2DZ levels are closer to the experimental values than those at the B3LYP/6-311+G(d)-LANL2DZ level and the former two methods give similar results (Table 2), and mainly BPW91/Aug-cc-PVTZ-LANL2DZ results are presented for discussions. The ground electronic states, point groups, vibrational frequencies, and intensities are listed in Table 3. Table 4 reports a comparison of the observed and calculated isotopic frequency ratios for the C–O stretching modes of the reaction products. Energetic analysis for possible reactions of Ag atoms with CO molecules is given in Table 5. Figure 5 shows the most stable structures of the reaction products.

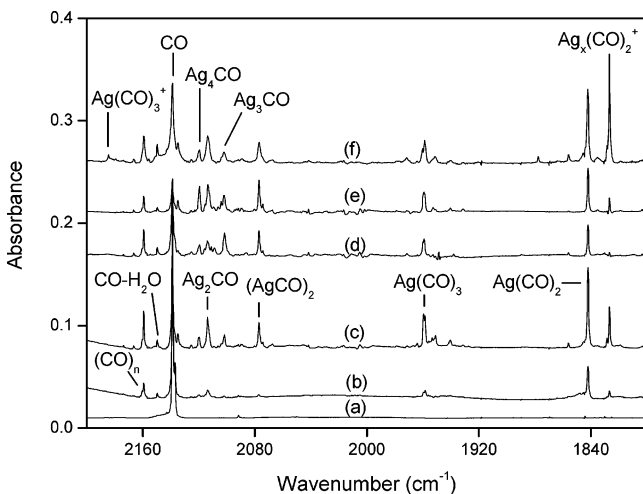
Ag(CO)₂ and Ag(CO)₃. The Ar matrix absorption at 1842.1 cm⁻¹ (Table 1 and Figure 1) is due to the antisymmetric C–O stretching vibration of the Ag(CO)₂ molecule, which is consistent with the previous reports of 1858.7 and 1842.0 cm⁻¹ absorptions in Ne and Ar,⁵ respectively. The 1959.5 cm⁻¹ band (Table 1 and Figure 1) is due to the doubly degenerate C–O stretching mode of the Ag(CO)₃ molecule. However, no absorption of AgCO has been observed in both neon and argon experiments. Detailed discussions about the mononuclear silver

TABLE 4: Comparison of the Observed and Calculated (at the BPW91/Aug-cc-PVTZ-LANL2DZ Level) Isotopic Frequency Ratios of the Possible Reaction Products

molecule	mode	$^{12}\text{C}^{16}\text{O}/^{13}\text{C}^{16}\text{O}$		$^{12}\text{C}^{16}\text{O}/^{12}\text{C}^{18}\text{O}$	
		obsd	calcd	obsd	calcd
$\text{Ag}(\text{CO})_2$	C–O str.	1.0228	1.0234	1.0237	1.0238
$\text{Ag}(\text{CO})_3$	C–O asym-str.	1.0227	1.0235	1.0238	1.0237
Ag_2CO	C–O str.	1.0227	1.0230	1.0240	1.0248
$(\text{AgCO})_2$	C–O asym-str.	1.0224	1.0228	1.0242	1.0248
$\text{AgAg}(\text{CO})_2$	C–O sym-str.		1.0233		1.0240
$\text{AgAg}(\text{CO})_2$	C–O asym-str.		1.0230		1.0243
Ag_3CO	C–O str.	1.0226	1.0234	1.0239	1.0239
Ag_4CO	C–O str.	1.0226	1.0233	1.0238	1.0240

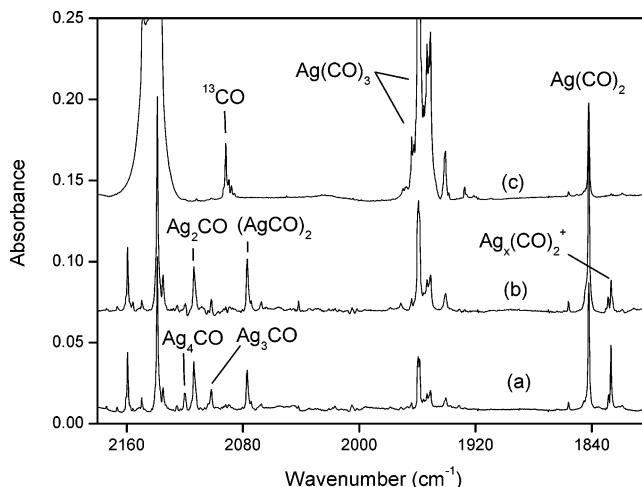
TABLE 5: Energetics for Possible Reactions of Silver Atoms with CO Calculated at the BPW91/Aug-cc-PVTZ-LANL2DZ Level

no.	reaction	reaction energy ^a (kcal/mol)
1	$\text{Ag}(^2\text{S}_{1/2}) + \text{Ag}(^2\text{S}_{1/2}) \rightarrow \text{Ag}_2(^1\Sigma_g^+)$	−37.26
2	$\text{Ag}_2(^1\Sigma_g^+) + \text{Ag}(^2\text{S}_{1/2}) \rightarrow \text{Ag}_3(^2\text{B}_2)$	−17.00
3	$\text{Ag}(^2\text{S}_{1/2}) + \text{Ag}_3(^2\text{B}_2) \rightarrow \text{Ag}_4(^1\text{A}_g)$	−40.94
4	$\text{Ag}_2(^1\Sigma_g^+) + \text{Ag}_2(^1\Sigma_g^+) \rightarrow \text{Ag}_4(^1\text{A}_g)$	−20.68
5	$\text{Ag}(^2\text{S}_{1/2}) + 2\text{CO}(^1\Sigma^+) \rightarrow \text{Ag}(\text{CO})_2(^2\text{A}_1)$	−19.17
6	$\text{Ag}(\text{CO})_2(^2\text{A}_1) + \text{CO}(^1\Sigma^+) \rightarrow \text{Ag}(\text{CO})_3(^2\text{A}_1)$	−8.57
7	$\text{Ag}_2(^1\Sigma_g^+) + \text{CO}(^1\Sigma^+) \rightarrow \text{Ag}_2\text{CO}(^1\text{A})$	−10.45
8	$\text{Ag}(\text{CO})_2(^2\text{A}_1) + \text{Ag}(^2\text{S}_{1/2}) \rightarrow (\text{AgCO})_2(^1\text{A}_g)$	−37.45
9	$\text{Ag}_2\text{CO}(^1\text{A}) + \text{CO}(^1\Sigma^+) \rightarrow (\text{AgCO})_2(^1\text{A}_g)$	−8.92
10	$\text{Ag}_3(^2\text{B}_2) + \text{CO}(^1\Sigma^+) \rightarrow \text{Ag}_3\text{CO}(^2\text{B}_2)$	−16.71
11	$\text{Ag}_2\text{CO}(^1\text{A}) + \text{Ag}(^2\text{S}_{1/2}) \rightarrow \text{Ag}_3\text{CO}(^2\text{B}_2)$	−23.26
12	$\text{Ag}_4(^1\text{A}_g) + \text{CO}(^1\Sigma^+) \rightarrow \text{Ag}_4\text{CO}(^1\text{A}_1)$	−17.71
13	$\text{Ag}_2\text{CO}(^1\text{A}) + \text{Ag}_2(^1\Sigma_g^+) \rightarrow \text{Ag}_4\text{CO}(^1\text{A}_1)$	−27.94
14	$\text{Ag}_3\text{CO}(^2\text{B}_2) + \text{Ag}(^2\text{S}_{1/2}) \rightarrow \text{Ag}_4\text{CO}(^1\text{A}_1)$	−41.94

^a A negative value of energy denotes that the reaction is exothermic.**Figure 1.** IR spectra in the 2160–1800 cm^{-1} region from co-deposition of laser-ablated (12 mJ/pulse) Ag atoms with 0.02% CO in Ar: (a) 1 h of sample deposition at 7 K, (b) after annealing to 25 K, (c) after annealing to 30 K, (d) after 15 min of broad-band irradiation, (e) after annealing to 35 K, and (f) 0.02% CO + 0.005% CCl_4 , after annealing to 30 K.

carbonyls have been reported previously,⁵ and we will focus on the small silver cluster carbonyls in this study.

(AgCO)₂. The absorption at 2077.0 cm^{-1} that appears on sample annealing changes little after broad-band irradiation and increases slightly upon further annealing, as shown in Figure 1. The 2077.0 cm^{-1} band shifts to 2031.4 cm^{-1} with $^{13}\text{C}^{16}\text{O}$, and to 2077.9 cm^{-1} with $^{12}\text{C}^{18}\text{O}$, exhibiting isotopic frequency ratios ($^{12}\text{C}^{16}\text{O}/^{13}\text{C}^{16}\text{O}$, 1.0224; $^{12}\text{C}^{16}\text{O}/^{12}\text{C}^{18}\text{O}$, 1.0242) characteristic of C–O stretching vibrations (Table 1 and Figure 3).

**Figure 2.** IR spectra in the 2160–1800 cm^{-1} region for laser-ablated Ag atoms co-deposited with different CO concentration and laser power after annealing to 30 K in Ar: (a) 0.02% CO and 12 mJ/pulse, (b) 0.03% CO and 10 mJ/pulse, and (c) 0.4% CO and 7 mJ/pulse.

As can be seen in Figure 3, a triplet at 2076.9, 2039.8, and 2031.4 cm^{-1} together with a weak associated band at 2123.6 cm^{-1} has been observed in the mixed $^{12}\text{C}^{16}\text{O} + ^{13}\text{C}^{16}\text{O}$ experiment, suggesting that two CO subunits are involved.³² A similar isotopic splitting feature has been obtained in the mixed $^{12}\text{C}^{16}\text{O} + ^{12}\text{C}^{18}\text{O}$ isotopic spectra (Figure 3). The IR spectra as a function of changes of CO concentrations and laser energies are of particular interest here. The $\text{Ag}(\text{CO})_n$ ($n = 2, 3$) molecules are the primary products at the experimental condition of high CO concentration (0.40%) and low laser energy (7 mJ/pulse) (Figure 2c), whereas the 2077.0 cm^{-1} band was produced at the experimental conditions of lower CO concentration (0.02%) and higher laser power (12 mJ/pulse) (Table 1 and Figure 2a). Doping with CCl_4 has no effect on this band (Figure 1f), suggesting that the product is neutral.³³ Furthermore, N_2 - or H_2O -doping exhibits no effect on the absorption at 2077.0 cm^{-1} (not shown here), indicating that N_2 and H_2O are not involved in the formation of this species. By analogy with $\text{Au}_2(\text{CO})_2^{5e,25}$ and $\text{M}_2(\text{CO})_2$ ($\text{M} = \text{Si}, \text{Ge}, \text{Sn}$) spectra,²⁴ the 2077.0 cm^{-1} band is assigned to the antisymmetric C–O stretching mode of $(\text{AgCO})_2$. The bands observed at 2123.6 cm^{-1} in the mixed $^{12}\text{C}^{16}\text{O} + ^{13}\text{C}^{16}\text{O}$ experiment and 2122.8 cm^{-1} in the $^{12}\text{C}^{16}\text{O} + ^{12}\text{C}^{18}\text{O}$ experiment are due to the symmetric C–O stretching modes of $\text{Ag}_2(^{12}\text{CO})(^{13}\text{CO})$ and $\text{Ag}_2(^{16}\text{O})(^{18}\text{O})$, respectively.

The assignment is strongly supported by the present DFT calculations. The $(\text{AgCO})_2$ molecule is predicted to have C_{2h} symmetry with an $^1\text{A}_g$ ground electronic state (Table 2 and Figure 5), which lies 38.14 kcal/mol in energy lower than a triplet state. The singlet and triplet $\text{AgAg}(\text{CO})_2$ isomers with C_{2v} symmetry are calculated to be 2.91 and 29.72 kcal/mol in energy higher than the singlet $(\text{AgCO})_2$, respectively. At the BPW91/Aug-cc-PVTZ-LANL2DZ level, the antisymmetric C–O stretching frequency in the singlet $(\text{AgCO})_2$ molecule is calculated to be 2037.1 cm^{-1} , which requires a 0.981 scale factor. The calculated $^{12}\text{C}^{16}\text{O}/^{13}\text{C}^{16}\text{O}$ and $^{12}\text{C}^{16}\text{O}/^{12}\text{C}^{18}\text{O}$ isotopic frequency ratios of 1.0228 and 1.0248 are again in good agreement with the experimental observations, 1.0224 and 1.0242, respectively. The symmetric and antisymmetric C–O stretching frequencies in the singlet $\text{AgAg}(\text{CO})_2$ isomer are predicted to be 2042.5 (469) and 2015.6 (1446 km/mol) cm^{-1} (Table 3), showing $^{12}\text{C}^{16}\text{O}/^{13}\text{C}^{16}\text{O}$ and $^{12}\text{C}^{16}\text{O}/^{12}\text{C}^{18}\text{O}$ isotopic frequency ratios of 1.0233 and 1.0230, 1.0240 and 1.0243 (Table 4), respectively, which do not match the observed patterns in the mixed isotopic spectra.

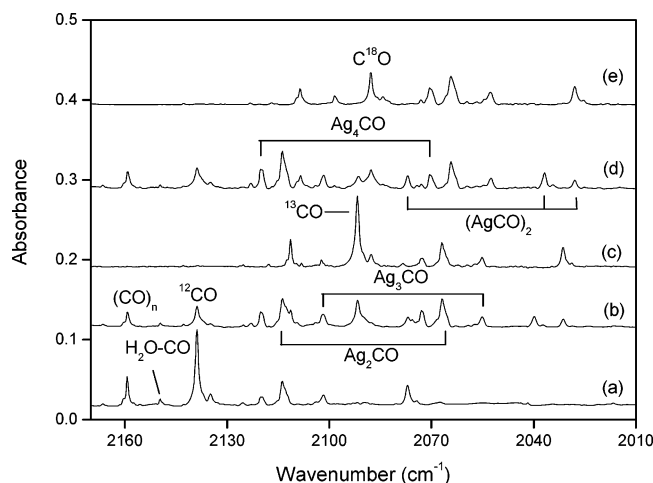


Figure 3. IR spectra in the 2160–2010 cm^{−1} region for laser-ablated (12 mJ/pulse) Ag atoms co-deposited with isotopic CO in Ar after annealing to 30 K: (a) 0.02% ¹²C¹⁶O, (b) 0.01% ¹²C¹⁶O + 0.01% ¹³C¹⁶O, (c) 0.02% ¹³C¹⁶O, (d) 0.01% ¹²C¹⁶O + 0.01% ¹²C¹⁸O, and (e) 0.02% ¹²C¹⁸O.

Ag_nCO (*n* = 2–4). The formation of small silver cluster carbonyls has also been observed in the present argon experiments. For instance, new absorptions at 2113.8, 2101.7, and 2119.8 cm^{−1} are observed upon sample annealing (Table 1 and Figure 1). As can be seen from Figure 2, the experimental condition of lower CO concentration and higher laser power favors the formation of these new bands, implying that these bands are attributed to polynuclear silver carbonyls.

The 2113.8, 2101.7, and 2119.8 cm^{−1} absorptions shift to 2066.9, 2055.2, and 2072.9 cm^{−1} with ¹³C¹⁶O and to 2064.3, 2052.7, and 2070.5 cm^{−1} with ¹²C¹⁸O, respectively. In the mixed ¹²C¹⁶O + ¹³C¹⁶O and ¹²C¹⁶O + ¹²C¹⁸O samples, only pure isotopic counterparts are observed. The isotopic ratios (¹²C¹⁶O/¹³C¹⁶O, 1.0227, 1.0226, and 1.0226; ¹²C¹⁶O/¹²C¹⁸O, 1.0240, 1.0239, and 1.0238, respectively) and the mixed isotopic characteristic (Figure 3) indicate that only one CO subunit is involved in each mode.³² It has been found that a high metal/CO ratio favors the formation of higher clusters during annealing.^{19–25} It can be seen from Figure 2 that the absorptions at 2113.8 (Ag₂CO) and 2077.0 cm^{−1} ((AgCO)₂) are more favored in the experiment of 0.03% CO with 10 mJ/pulse (Figure 2b), whereas the 2101.7 and 2119.8 cm^{−1} bands are more favored in the experimental conditions of lower CO concentration (0.02%) and higher laser power (12 mJ/pulse) (Figure 2a). Doping with CCl₄ has no effect on these bands (Figure 1f), suggesting that the products are neutral.³³ Furthermore, N₂- or H₂O-doping exhibits no effect on these absorptions (not shown here), which excludes the effect of N₂ and H₂O to the formation of the products. By analogy with spectra previously reported for Au_nCO (*n* = 1–5) and M_nCO (M = Si, Ge, Pb; *n* = 2–5),^{5e,24,25} the 2113.8, 2101.7, and 2119.8 cm^{−1} bands are assigned to the C–O stretching vibrations of small silver cluster Ag_nCO (*n* = 2–4) carbonyls, respectively, based on the results of the isotopic substitution and the CO concentration change and the comparison with theoretical predictions (Tables 2–4) (vide infra).

It can be seen that the calculated frequencies and the isotopic frequency ratios are in good agreement with the experimental values (Tables 1 and 2). As shown in Figure 5, a terminal CO has been found in the most stable structures of Ag₂CO, Ag₃CO, and Ag₄CO, which is consistent with the recent DFT predictions.^{12c}

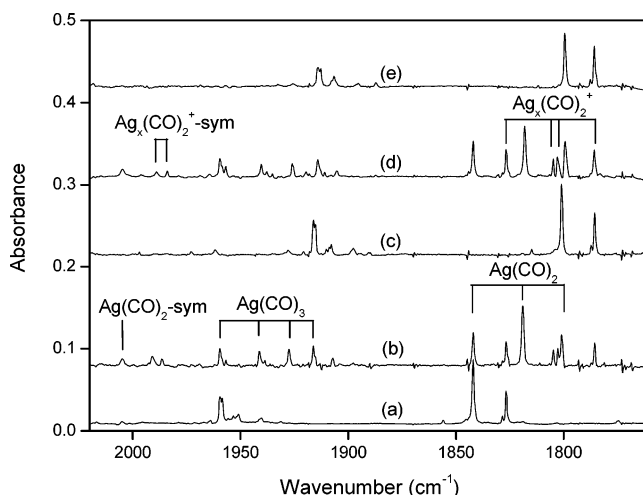


Figure 4. IR spectra in the 2100–1780 cm^{−1} region for laser-ablated (12 mJ/pulse) Ag atoms co-deposited with isotopic CO in Ar after annealing to 30 K: (a) 0.02% ¹²C¹⁶O, (b) 0.01% ¹²C¹⁶O + 0.01% ¹³C¹⁶O, (c) 0.02% ¹³C¹⁶O, (d) 0.01% ¹²C¹⁶O + 0.01% ¹²C¹⁸O, and (e) 0.02% ¹²C¹⁸O.

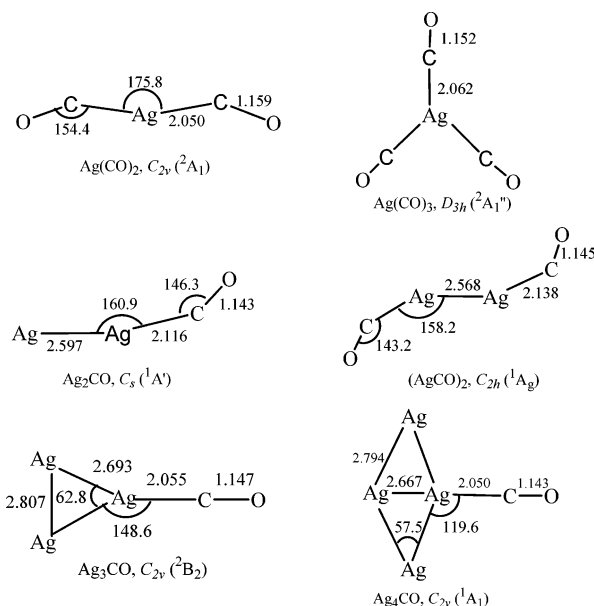


Figure 5. Optimized structures (bond lengths in angstroms, bond angles in degrees) of the most stable isomers for the reaction products calculated at the BPW91/Aug-cc-PVTZ-LANL2DZ level.

The present optimized Ag–Ag distance in the naked Ag₂ cluster is 2.585 Å, in accord with the experimental value (2.531 Å)^{11b} and the previous VWN calculations (2.504 Å).¹² The Ag–Ag stretching of the Ag₂ cluster is IR inactive, but the vibrational frequency of Ag₂ in the gas phase was observed at 192 cm^{−1}.³⁴ A harmonic frequency of the Ag₂ cluster is calculated to be 185.4 cm^{−1} at the BPW91/Aug-cc-PVTZ-LANL2DZ level, which is beyond the present spectral range of 5000–400 cm^{−1}. The present DFT calculations predict that Ag₂CO has an asymmetric structure with an ¹A' ground state (Table 2 and Figure 5), which lies 39.80 kcal/mol in energy lower than a triplet state. The singlet and triplet AgCOAg isomers are predicted to be 50.00 and 41.31 kcal/mol in energy higher than the singlet Ag₂CO, respectively. The Ag–C bond length and the AgAgC angle in the singlet Ag₂CO are calculated to be 2.116 Å and 160.9°, respectively. For Ag₂CO, the Ag–Ag bond length is 2.597 Å, which is 0.012 Å longer than that of ligand-free Ag₂.

The naked Ag_3 cluster has a $^2\text{B}_2$ ground state with C_{2v} symmetry, which is in accordance with the previous studies.¹² The calculated results predict that Ag_3CO has a $^2\text{B}_2$ ground state with a terminal CO, which lies 65.68 kcal/mol in energy lower than a quartet state. In Ag_3CO , the apex angle is predicted to be 62.8° (Figure 5).

For Ag_4 , a planar rhombus arrangement with D_{2h} symmetry in the $^1\text{A}_g$ ground state is the most stable structure, which is in agreement with the previous studies.¹² The most stable structure of Ag_4CO is predicted to have an $^1\text{A}_1$ ground state with a planar geometry of C_{2v} symmetry, which lies 21.68 kcal/mol in energy lower than a triplet state. The CO molecule is terminally bonded to one of the apex Ag atoms near the rhombus Ag_4 . The CAgAg angle is calculated to be 119.6° . In contrast, Au_4CO was predicted to have a planar structure with C_s symmetry, in which CO is terminally bonded to one of the apex Au atoms of the triangle Au_3 ring.²⁵

Other Absorptions. The absorption at 1826.7 cm^{-1} is favored by higher laser energy (Table 1, Figures 1 and 2) and is due to higher polynuclear silver carbonyls. A quartet pattern has been observed in the mixed $^{12}\text{C}^{16}\text{O} + ^{13}\text{C}^{16}\text{O}$ and $^{12}\text{C}^{16}\text{O} + ^{12}\text{C}^{18}\text{O}$ isotopic spectra. Doping with CCl_4 sharply enhances this band (Figure 1f), suggesting that the product is cationic.³³ This band is tentatively assigned to $\text{Ag}_x(\text{CO})_2^+$ containing two inequivalent COs.

Reaction Mechanism. With low CO concentrations and high laser energies, the laser-ablated silver atoms react with CO molecules in the excess argon matrix to produce the small silver cluster carbonyls, $(\text{AgCO})_2$ and Ag_nCO ($n = 2-4$), as well as $\text{Ag}(\text{CO})_n$ ($n = 2, 3$) (Figure 1).

Under the present experimental conditions, silver atoms are the predominant species produced by laser ablation of the silver target. As shown in Figure 1, the $(\text{AgCO})_2$ and Ag_nCO ($n = 2-4$) species appear upon sample annealing and increase significantly upon further annealing to high temperatures (30–35 K) in the experiments with low CO concentrations, which indicates that these small silver clusters are mainly formed in solid argon upon annealing but not during the laser ablation process. This means that the higher laser power leads neither to generating more clusters in the gas phase nor to significant annealing of the matrix during deposition therefore increasing the yield of the Ag_n species. It seems that a higher laser power accounts for the generation of a higher concentration of Ag in the matrix, corresponding to a higher Ag/CO ratio.

The energetic analysis for possible reactions of silver atoms and small clusters with CO molecules has been performed at the BPW91/Aug-cc-PVTZ-LANL2DZ level. As can be seen in Table 5, all the possible reactions of silver atoms and small clusters with CO are exothermic (-17.00 to -40.94 kcal/mol). This implies that the diffusion during annealing may make a species, for example, a silver atom or cluster, a CO molecule, or a silver carbonyl intermediate, in the matrix readily react with its nearest neighbor, and consequently, the final product distribution will mainly depend on the Ag/CO ratio; this is in agreement with our observations that low CO concentration and high laser power favor high nuclearity of cluster molecules (Figure 2). In contrast, at a high CO concentration and low laser power, corresponding to a low Ag/CO ratio, mononuclear silver di- and tricarbonyl species are the predominant products.

Conclusion

Laser-ablated silver atoms react with carbon monoxide molecules in the excess argon and neon matrices to produce metal carbonyl species. In addition to the previously reported

mononuclear silver carbonyls, small silver cluster carbonyls, $(\text{AgCO})_2$ and Ag_nCO ($n = 2-4$), have been observed in the present argon experiments but absent from the neon experiments. On the basis of the results of the isotopic substitution, stepwise annealing, change of CO concentration and laser energy, and the comparison with theoretical predictions, the absorption at 2077.0 cm^{-1} has been assigned to $(\text{AgCO})_2$ and the absorptions at 2113.8 , 2101.7 , and 2119.8 cm^{-1} have been assigned to Ag_2CO , Ag_3CO , and Ag_4CO , respectively. The present study reveals that CO is terminally bonded in these small silver cluster carbonyls. The observation of $(\text{AgCO})_2$ and Ag_nCO ($n = 2-4$) is in good agreement with the prediction of DFT calculations.

Acknowledgment. We gratefully acknowledge financial support for this research by a Grant-in-Aid for Scientific Research (B) (Grant No. 17350012) from the Ministry of Education, Culture, Sports, Science and Technology (MEXT) of Japan. L.J. thanks MEXT of Japan and Kobe University for an Honors Scholarship.

References and Notes

- (1) Kilty, P. A.; Sachtler, W. M. H. *Catal. Rev.-Sci. Eng.* **1974**, *10*, 1 and references therein. Heiz, U.; Schneider, W. D. In *Metal Clusters at Surfaces*; Meiwes-Broer, K. H., Ed.; Springer-Verlag: Berlin, Germany, 2000.
- (2) See, for example: Mostafavi, M.; Marignier, J. L.; Amblard, J.; Belloni, J. *Radiat. Phys. Chem.* **1989**, *34*, 605. Eachus, R. S.; Marchetti, A. P.; Muentner, A. A. *Annu. Rev. Phys. Chem.* **1999**, *50*, 117.
- (3) Kim, S. H.; Medeiros-Ribeiro, G.; Ohlberg, D. A. A.; Williams, R. S.; Heath, J. R. *J. Phys. Chem. B* **1999**, *103*, 10341.
- (4) McIntosh, D.; Ozin, G. A. *Inorg. Chem.* **1976**, *15*, 2869; **1977**, *16*, 59. Chertihin, G. V.; Andrews, L.; Bauschlicher, C. W., Jr. *J. Phys. Chem. A* **1997**, *101*, 4026. Wang, X. F.; Andrews, L. *J. Phys. Chem. A* **2001**, *105*, 5812. Citra, A.; Andrews, L. *J. Mol. Struct. (THEOCHEM)* **1999**, *189*, 95.
- (5) See, for example: (a) McIntosh, D.; Ozin, G. A. *J. Am. Chem. Soc.* **1976**, *98*, 3167. (b) Kasai, P. H.; Jones, P. M. *J. Phys. Chem.* **1985**, *89*, 1147. (c) Kasai, P. H.; Jones, P. M. *J. Am. Chem. Soc.* **1985**, *107*, 6385. (d) Marian, C. M. *Chem. Phys. Lett.* **1993**, *215*, 582. (e) Liang, B.; Andrews, L. *J. Phys. Chem. A* **2000**, *104*, 9156.
- (6) Hurlburt, P. K.; Anderson, O. P.; Strauss, S. H. *J. Am. Chem. Soc.* **1991**, *113*, 6277. Hurlburt, P. K.; Rack, J. J.; Dec, S. F.; Anderson, O. P.; Strauss, S. H. *Inorg. Chem.* **1993**, *32*, 373. Hurlburt, P. K.; Rack, J. J.; Luck, J. S.; Dec, S. F.; Webb, J. D.; Anderson, O. P.; Strauss, S. H. *J. Am. Chem. Soc.* **1994**, *116*, 10003.
- (7) Rack, J. J.; Moasser, B.; Gargulak, J. D.; Gladfelter, W. L.; Hochheimer, H. D.; Strauss, S. H. *J. Chem. Soc., Chem. Commun.* **1994**, 685. Rack, J. J.; Polyakov, O. G.; Gaudinski, C. M.; Hammel, J. W.; Kasperbauer, P.; Hochheimer, H. D.; Strauss, S. H. *Appl. Spectrosc.* **1998**, *52*, 1035.
- (8) Willner, H.; Aubke, F. *Inorg. Chem.* **1990**, *29*, 2195. Willner, H.; Schaebs, J.; Hwang, G.; Mistry, F.; Jones, R.; Trotter, J.; Aubke, F. *J. Am. Chem. Soc.* **1992**, *114*, 8972.
- (9) Tsumori, N.; Xu, Q.; Hirahara, M.; Tanihata, S.; Souma, Y.; Nishimura, Y.; Kuriyama, N.; Tsubota, S. *Bull. Chem. Soc. Jpn.* **2002**, *75*, 2257.
- (10) Xu, Q.; Jiang, L. *J. Phys. Chem. A* **2006**, *110*, 2655.
- (11) (a) Ozin, G. A.; Huber, H. *Inorg. Chem.* **1978**, *17*, 155. (b) Simard, B.; Hackett, P. A.; James, A. M.; Langridge-Smith, P. R. *Chem. Phys. Lett.* **1991**, *186*, 415.
- (12) (a) Fournier, R. *J. Chem. Phys.* **2001**, *115*, 2165. (b) Zhao, S.; Li, Z.-H.; Wang, W.-N.; Liu, Z.-P.; Fan, K.-N.; Xie, Y.; Schaefer, H. F., III. *J. Chem. Phys.* **2006**, *124*, 184102. (c) Zhou, J.; Li, Z.-H.; Wang, W.-N.; Fan, K.-N. *J. Phys. Chem. A* **2006**, *110*, 7167.
- (13) Varga, S.; Fricke, B.; Nakamatsu, H.; Mukoyama, T.; Anton, J.; Geschke, D.; Heitmann, A.; Engel, E.; Bastug, T. *J. Chem. Phys.* **2000**, *112*, 3499.
- (14) Cotton, F. A.; Wilkinson, G.; Murillo, C. A.; Bochmann, M. *Advanced Inorganic Chemistry*, 6th ed.; Wiley: New York, 1999.
- (15) Lupinetti, A. J.; Strauss, S. H.; Frenking, G. *Prog. Inorg. Chem.* **2001**, *49*, 1. Willner, H.; Aubke, F. *Chem.-Eur. J.* **2003**, *9*, 1669. Xu, Q. *Coord. Chem. Rev.* **2002**, *231*, 83.
- (16) Rabin, I.; Schulze, W. *J. Phys. Chem. B* **2004**, *108*, 14575.
- (17) See, for example: Xu, C.; Manceron, L.; Perchard, J. P. *J. Chem. Soc., Faraday Trans.* **1993**, *89*, 1291. Bondybey, V. E.; Smith, A. M.; Agreiter, J. *Chem. Rev.* **1996**, *96*, 2113. Fedrigo, S.; Haslett, T. L.; Moskovits, M. *J. Am. Chem. Soc.* **1996**, *118*, 5083. Khriachtchev, L.; Pettersson, M.; Runeberg, N.; Lundell, J.; Rasanen, M. *Nature* **2000**, *406*,

874. Himmel, H. J.; Manceron, L.; Downs, A. J.; Pullumbi, P. *J. Am. Chem. Soc.* **2002**, *124*, 4448. Li, J.; Bursten, B. E.; Liang, B.; Andrews, L. *Science* **2002**, *295*, 2242. Andrews, L.; Wang, X. *Science* **2003**, *299*, 2049.
- (18) (a) Zhou, M. F.; Tsumori, N.; Li, Z.; Fan, K.; Andrews, L.; Xu, Q. *J. Am. Chem. Soc.* **2002**, *124*, 12936. (b) Zhou, M. F.; Xu, Q.; Wang, Z.; von Ragué Schleyer, P. *J. Am. Chem. Soc.* **2002**, *124*, 14854. (c) Jiang, L.; Xu, Q. *J. Am. Chem. Soc.* **2005**, *127*, 42.
- (19) Zhou, M. F.; Chertihin, G. V.; Andrews, L. *J. Chem. Phys.* **1998**, *109*, 10893. Zhou, M. F.; Andrews, L. *J. Chem. Phys.* **1999**, *110*, 10370. Tremblay, B.; Gutsev, G.; Manceron, L.; Andrews, L. *J. Phys. Chem. A* **2002**, *106*, 10525.
- (20) Tremblay, B.; Manceron, L.; Gutsev, G.; Andrews, L.; Partridge, H., III. *J. Chem. Phys.* **2002**, *117*, 8479.
- (21) Zhou, M. F.; Wang, Z. X.; Schleyer, P. v. R.; Xu, Q. *ChemPhysChem* **2003**, *4*, 763. Zhou, M. F.; Tsumori, N.; Li, Z. H.; Fan, K. N.; Andrews, L.; Xu, Q. *J. Am. Chem. Soc.* **2002**, *124*, 12936.
- (22) Jiang, L.; Xu, Q. *J. Phys. Chem. A* **2006**, *110*, 5636.
- (23) Xu, Q.; Jiang, L.; Tsumori, N. *Angew. Chem., Int. Ed.* **2005**, *44*, 4338.
- (24) Zhou, M. F.; Jiang, L.; Xu, Q. *J. Chem. Phys.* **2004**, *121*, 10474.
- (b) Zhou, M. F.; Jiang, L.; Xu, Q. *J. Phys. Chem. A* **2005**, *109*, 3325. (c) Jiang, L.; Xu, Q. *Bull. Chem. Soc. Jpn.* **2006**, *79*, 857. (d) Jiang, L.; Xu, Q. *J. Chem. Phys.* **2005**, *122*, 034505.
- (25) Jiang, L.; Xu, Q. *J. Phys. Chem. A* **2005**, *109*, 1026.
- (26) Burkholder, T. R.; Andrews, L. *J. Chem. Phys.* **1991**, *95*, 8697.
- (27) Zhou, M. F.; Tsumori, N.; Andrews, L.; Xu, Q. *J. Phys. Chem. A* **2003**, *107*, 2458.
- (28) Frisch, M. J.; Trucks, G. W.; Schlegel, H. B.; Scuseria, G. E.; Robb, M. A.; Cheeseman, J. R.; Montgomery, J. A., Jr.; Vreven, T.; Kudin, K. N.; Burant, J. C.; Millam, J. M.; Iyengar, S. S.; Tomasi, J.; Barone, V.; Mennucci, B.; Cossi, M.; Scalmani, G.; Rega, N.; Petersson, G. A.; Nakatsuji, H.; Hada, M.; Ehara, M.; Toyota, K.; Fukuda, R.; Hasegawa, J.; Ishida, M.; Nakajima, T.; Honda, Y.; Kitao, O.; Nakai, H.; Klene, M.; Li, X.; Knox, J. E.; Hratchian, H. P.; Cross, J. B.; Adamo, C.; Jaramillo, J.; Gomperts, R.; Stratmann, R. E.; Yazyev, O.; Austin, A. J.; Cammi, R.; Pomelli, C.; Ochterski, J. W.; Ayala, P. Y.; Morokuma, K.; Voth, G. A.; Salvador, P.; Dannenberg, J. J.; Zakrzewski, V. G.; Dapprich, S.; Daniels, A. D.; Strain, M. C.; Farkas, O.; Malick, D. K.; Rabuck, A. D.; Raghavachari, K.; Foresman, J. B.; Ortiz, J. V.; Cui, Q.; Baboul, A. G.; Clifford, S.; Cioslowski, J.; Stefanov, B. B.; Liu, G.; Liashenko, A.; Piskorz, P.; Komaromi, I.; Martin, R. L.; Fox, D. J.; Keith, T.; Al-Laham, M. A.; Peng, C. Y.; Nanayakkara, A.; Challacombe, M.; Gill, P. M. W.; Johnson, B.; Chen, W.; Wong, M. W.; Gonzalez, C.; Pople, J. A. *Gaussian 03*, revision B.04; Gaussian, Inc.: Pittsburgh, PA, 2003.
- (29) Lee, C.; Yang, E.; Parr, R. G. *Phys. Rev. B* **1988**, *37*, 785. Becke, A. D. *J. Chem. Phys.* **1993**, *98*, 5648. Becke, A. D. *Phys. Rev. A* **1988**, *38*, 3098. Perdew, J. P.; Burke, K.; Wang, Y. *Phys. Rev. B* **1996**, *54*, 16533.
- (30) McLean, A. D.; Chandler, G. S. *J. Chem. Phys.* **1980**, *72*, 5639. Krishnan, R.; Binkley, J. S.; Seeger, R.; Pople, J. A. *J. Chem. Phys.* **1980**, *72*, 650. Frisch, M. J.; Pople, J. A.; Binkley, J. S. *J. Chem. Phys.* **1984**, *80*, 3265. Kendall, R. A.; Dunning, T. H., Jr.; Harrison, R. J. *J. Chem. Phys.* **1992**, *96*, 6796.
- (31) Hay, P. J.; Wadt, W. R. *J. Chem. Phys.* **1985**, *82*, 299.
- (32) Darling, J. H.; Ogden, J. S. *J. Chem. Soc., Dalton Trans.* **1972**, 2496.
- (33) Zhou, M. F.; Andrews, L.; Bauschlicher, C. W., Jr. *Chem. Rev.* **2001**, *101*, 1931 and references therein.
- (34) Huber, K. P.; Herzberg, G. *Molecular Spectra and Molecular Structure, Constants of Diatomic Molecules*; Van Nostrand: Toronto, Canada, 1979; Vol. IV.